2019

Adaptive hybrid structures to enhance graphene-based sensors for detecting moisture in corn plants

Matthew Davis
Iowa State University

Adaptive hybrid structures to enhance graphene-based sensors for detecting moisture in corn plants

by

Matthew Davis

A thesis submitted to the graduate faculty

in partial fulfillment of the requirements for the degree of

MASTER OF SCIENCE

Major: Electrical Engineering

Program of Study Committee:
Liang Dong, Major Professor
Meng Lu
Jiming Song

The student author, whose presentation of the scholarship herein was approved by the program of study committee, is solely responsible for the content of this thesis. The Graduate College will ensure this thesis is globally accessible and will not permit alterations after a degree is conferred.

Iowa State University

Ames, Iowa

2019

TABLE OF CONTENTS

ABSTRACT

The utilization of graphene, a two-dimensional structure of carbon atoms, to measure water content in corn plants is presented. Discussed are the structural properties of graphene, fabrication methods, and previous designs by other research groups. This work attempts to design and test a new style of graphene sensor that maintains signal stability while not inhibiting plant growth or health. Specifically, the use of inkjet printing and molds to manufacture the graphene sensor component and the use of a soft polymer for a flexible attachment is examined. Simulations for determining the efficacy of mechanical structures are also analyzed.

CHAPTER 1. INTRODUCTION

Background

Plant Genomics

A major driving force in the agriculture industry is the study of plant genomics where the goal is to improve upon existing crops to make them stronger and more efficient. When analyzing these genetic changes, it is critical to perform various biological studies to characterize the phenotype effects. Without accurate data, it is difficult to understand gene interactions or any definitive conclusions on the gene strains in question.

Plant Transpiration

With the rise in global population and decrease of water availability, it becomes increasingly important for crops to be drought resistant and to have high water efficiency [1]. In general, this plant trait is controlled by the transpiration cycle and due to its importance it is one of the biological processes studied in plant genomics [1,2]. Transpiration is a multistep process of water uptake at the root level of the plant, followed by transportation of water through the plant, and ending with the release and evaporation of that water at its stomata [3]. This process occurs alongside photosynthesis as the stomata open to allow the intake of carbon dioxide gas. It also helps to cool plants, much like animal perspiration, and facilitates the flow of nutrients throughout the plant [3].

Measuring Transpiration

As with most biological processes, there are numerous ways to measure plant transpiration. The most rudimentary methods involve comparing weights, which are taken from a potted plant or a receptacle used to collect moisture from the leaves, and calculating the difference [4]. The difference roughly translates to the amount of moisture that was evaporated by the plant. While simple, these types of methods are generally inaccurate and

outdated. In modern work, the transpiration process is measured through more precise means. In general, these modern systems consist of input and output chambers surrounding the sample where humidity sensors measure the air humidity before reaching the plant leaf and after. For the humidity sensor itself, some industries use lithium chloride dew cells, Dunmore cells, and various resistive sensors made from carbon structures [5]. These sensors can measure local relative humidity in small chambers, but can be slow and temperature dependent [5]. Other methods utilize infrared lasers for measuring infrared absorption, which indicate water vapor pressure within the air chamber [5,6]. Lastly, transpiration at the stomata region can be measured using graphene sensors that take advantage of the material's carbon structure. This method is further explored in this work.

Purpose

The goal of this research is to design and manufacture an improved water sensor for corn plants to determine water uptake, retention, and expulsion characteristics for various genetic strains. This is done through a graphene-based sensor, which has a variable resistance depending upon the humidity near the detection region. Mechanically, it is shown that vapors and gasses are able to disperse within graphene layers due to its aromatic structure [7]. These non-graphene molecular groups can then alter the electrically conductive paths through the graphene, resulting in a change of measured resistance. This information, along with known humidity values, is then used to calibrate the graphene sensors.

One major issue with applying sensing technology to a subject is that it can interfere with the subject's ability to function normally. Previously, Oren et al. designed a tape-based graphene sensor that attached directly to the underside of a plant leaf to measure the water transpiration through the plant's stomata [8]. This design, while being simple and effective, also has a couple of potential issues. For one, the tape substrate is unable to expand,

potentially limiting the leaf's natural growth cycle. In addition, the tape curves with the leaf, which is good from a contact perspective, but also leads to deformation of the graphene sheets and changes to the baseline signal. The new device has two major goals. One is to provide a stable base for the graphene sensing component to reduce any mechanical changes that may occur. The second is to utilize a flexible material that serves as an intermediary between the main device and the plant leaf.

Sensing Component

Graphene is the material used for the primary sensing component of the device. There are two methods used for preparing graphene solutions since the different methods of fabricating sensors required different solution properties. The first mixture is prepared in a seventy percent ethanol and thirty percent deionized water solution. Graphene flakes are added so that there are 20 milligrams for every milliliter of solution. This mixture is sealed and then sonicated at room temperature for three hours to fully disperse the graphene particles. The second mixture is prepared in a seventy-five percent deionized water and twenty-five percent acetone solution with no ethanol, and contains only 10 milligrams of graphene flakes per milliliter.

Device Design

The sensor device itself is made of two different parts. The first is a base and cap structure made of rigid substrates, which provide mechanical and electrical stability, and the second is a soft polymer attachment that allows for leaf growth during the sensing period. These components also work together to maintain signal stability while separating the potentially damaged leaf binding site from the sensing area.

CHAPTER 2. LITERATURE REVIEW

Overview of Graphene

Graphene is the formation of bonded carbon atoms in a hexagonal lattice structure that exists as a two-dimensional plane. As such it is an aromatic molecule with no limit on overall size [9]. This material is interesting in many applications such as electronic, thermal, and mechanical due to its high strength and conductivities [9,10]. Originally graphene was only found due to graphite applications to metal surfaces, but was finally characterized by Geim and Novoselov in 2004 at the University of Manchester [11].

Fabrication of Graphene

General scientific experience shows that nanostructures are highly sensitive to production method since certain processes can create defects or non-ideal molecular structures. Graphene, with its nanoscale two-dimensional structure, is shown to have varying levels of conductivity based on its fabrication method.

Exfoliation of Graphite

One exfoliation based method of graphene production stems from micromechanical cleavage of graphite. In this method, graphene sheets of varying thickness are separated from graphite crystal by rubbing crystals against each other or by the use of an adhesive structure [12]. Since this process produces graphene of varying number of layers, the issue becomes one of identifying the single-layer graphene sheets. Currently, optical microscopes and Raman spectroscopy have shown the ability to identify layer thickness [12].

Another method of exfoliation utilizes organic liquids. This process is based on using a layered graphite structure that allows for a high concentration of surface area reactive sites. With a small liquid-to-graphite reactive distance, the overall interaction energy is low enough

for mechanical stimulation to break apart the graphite [12]. Essentially, the sonication and centrifugation of graphite in an active organic liquid results in the suspension of single-layer graphene sheets in the solution. This process works with numerous surface-active substances such as N-poly-methylpirrolidon (NMP), N,N-dimethylacetamide (DMA), g-buthyrolactone (GBL), and 1,3-dimethyl-2-imidasolidinon (DMEU) [12].

Oxidation of Graphite

Another approach to graphite layer exfoliation involves the use of chemical oxidizers [12]. In this method, inner graphite layers are oxidized as a result strong gaseous oxidizers such as oxygen and various halogens. As the graphite oxidizes, there is an increase in the interlayer distance in the crystal and as a result a decrease in the interlayer interaction energy. With a lower layer interaction energy, the oxidized graphite is easier to separate using liquid exfoliation to create graphene oxide sheets [12]. The most common approach to graphite oxidation is known as the Hummers method, which uses sulfuric acid, sodium nitrate, and potassium permanganate [12].

Chemical Vapor Deposition of Graphene

It is also possible to deposit graphene on various substrates through the use of chemical vapor deposition (CVD) [13]. In this process, the metal substrate is exposed to a hydrocarbon gas under low pressure or ultrahigh vacuum conditions. Different graphene thicknesses are achieved by varying the exposure time. For example, Reina et al. exposed polycrystalline nickel substrates to a highly diluted hydrocarbon flow under ambient pressure conditions [13]. They were able to achieve graphene films that were between one and ten layers thick on the nickel surface [13]. Another group, Kim et al. applied a film to a silicon dioxide / silicon substrate using a gaseous mixture of CH_4:H_2:Ar flowing at a ratio of

50:65:200 at 1000 °C [12]. When the synthesis reaction completed, the substrates were cooled down to room temperature at a rate of 10 °C per second under just an argon gas flow. Their experience showed that rapid cooling was critical in preventing the graphene sheets from agglomerating [12].

Epitaxial Growth of Graphene

Groups such as Berger et al. have shown that it is possible to fabricate graphene sensors using epitaxy [14]. For this process to work, a substrate with a highly-ordered crystalline structure is needed. When exposed to carbon at high temperatures, the substrate becomes saturated with carbon molecules across its entire volume [12]. As the metal is slowly cooled, the carbon solubility drastically decreases causing the release of carbon on the metal surface creating large islands of thin film graphene [12].

Graphene as a Moisture Sensor

Smith et al. created graphene humidity sensors on a silicon substrate in order to test the sensors ability to differentiate humidity in various gaseous environments [15]. The sensors used consisted of single layer graphene that was transitioned to a silicon dioxide substrate and then etched into regions 44 micrometers long and 80 micrometers wide [15]. For testing, Smith et al. utilized two chambers in order to cover a relative humidity range of 1% to 96% [12]. The lower relative humidity levels were achieved in a vacuum chamber and levels above 30% were done in a humidity chamber, which provided control over humidity levels at atmospheric pressure [15]. Prior to the humidity tests, the sensors were first exposed to dry argon, dry nitrogen, and then dry oxygen to observe any potential change in the output resistance. Smith et al. found that the signal was relatively stable and saw the most change

when water vapor was introduced or removed from the chamber, indicating a high specificity for humidity detection [15].

Another method of humidity detection using graphene was explored by Chen et al. Their proposal was that bilayer graphene promotes the opening of the molecular bandgap compared to single-layer graphene, and as a result, bilayer graphene is better suited for various device applications such as humidity sensing [16]. This sensor was manufactured by chemical vapor deposition of CH_4 onto copper foil in the presence of hydrogen gas. When the process was finished, Chen et al. transferred the sensor to a glass substrate and applied printed silver plastic as the electrode contacts for the measurement equipment [16]. Their results indicated that the measured current across the sensor with a 1.0 V bias increased by about 18 percent when in the presence of 98 percent humidity compared to the baseline case of 44 percent humidity [16]. Overall their data indicated a relatively strong linear trend with an R^2 value of 0.977 [16]. Chen et al. note that typical humidity sensors have a response time of around a couple of seconds, whereas this bilayer graphene humidity sensor demonstrates a response time in the millisecond range [16].

Graphene sensors can also be used in a capacitive state to measure relative humidity as shown by Zhang et al. [17]. In this research, Zhang et al. produced a graphene oxide and diallyldimethylammonium chloride (PDDA) nanocomposite film through a layer-by-layer assembly method [17]. The advantage of using graphene oxide as opposed to base graphene, according the Zhang et al. is that the oxygen functional groups on the surface edges increase the material's hydrophilicity and as such improve its overall sensitivity to water molecules [17]. The sensor was fabricated on a polyimide substrate with a layer of nickel/copper interdigital electrodes. Zhang et al. then layered two bi-layers of PDDA and poly-(sodium 4-

styrenesulfonate) (PSS) as precursor for charge enhancement. Lastly, they layered five bi-layers of graphene oxide and PDDA [17]. To test the sensor, Zhang et al. exposed it to various mixtures of aqueous solutions in a closed environment at 25 °C to simulate relative humidity values from 11 percent up to 97 percent. During these tests, they measured the capacitance of the sensor and found that the capacitance increases with increased relative humidity due to the absorption of water molecules to the surface [17].

CHAPTER 3. METHODS AND MATERIALS

Graphene Sensor Fabrication

Graphene Solution Preparation

There are two main solutions of graphene used depending on the method of deposition. The first solution is prepared in a seventy percent ethanol and thirty percent deionized water solution. Pre-purchased graphene flakes from the Graphene Supermarket are added so that there are 20 milligrams for every milliliter of solution. This mixture is sealed and then sonicated at room temperature for three hours to fully disperse the graphene particles. An ethanol-based solution enhances the mixture's graphene dispersion, which means increasing the graphene-to-liquid ratio, and it also improves the evaporation rate [8]. In some applications and deposition methods, like molded graphene fabrication, it is beneficial to have a quick evaporation rate.

In other methods such as inkjet printing, it is better to have a slower evaporation rate so as to not induce evaporation during ink jetting. For this, a second graphene solution is prepared using deionized water and acetone in a three to one ratio. Pure deionized water was initially used as the mixture, but it created blotting in the printed pattern due to the water's relatively high surface tension. The inclusion of acetone assisted in lowering the overall surface tension, allowing for more even printed layers. Also, without the ethanol, graphene has poorer dispersion and so only 10 milligrams per milliliter is used. Similar to the ethanol solution, this one is initially sonicated at room temperature for three hours, but also requires a shorter sonication period prior to each use to re-disperse the graphene flakes.

Methods of Deposition

A handful of different graphene deposition methods are attempted, while only one of them is used for final sensor fabrication. During early device designs, the ethanol-based

graphene solution was deposited onto a methacrylic acid ester based polymer substrate using a syringe. This was done both directly to the substrate with no other material guiding the droplet shape or position and also with a POLYMER ring that acted as a mold or cast (figure 1). It was found that this method did not produce high quality graphene sheets and would therefore require high temperature annealing. However, the substrate material is unable to withstand the needed annealing temperature of 200 °C.

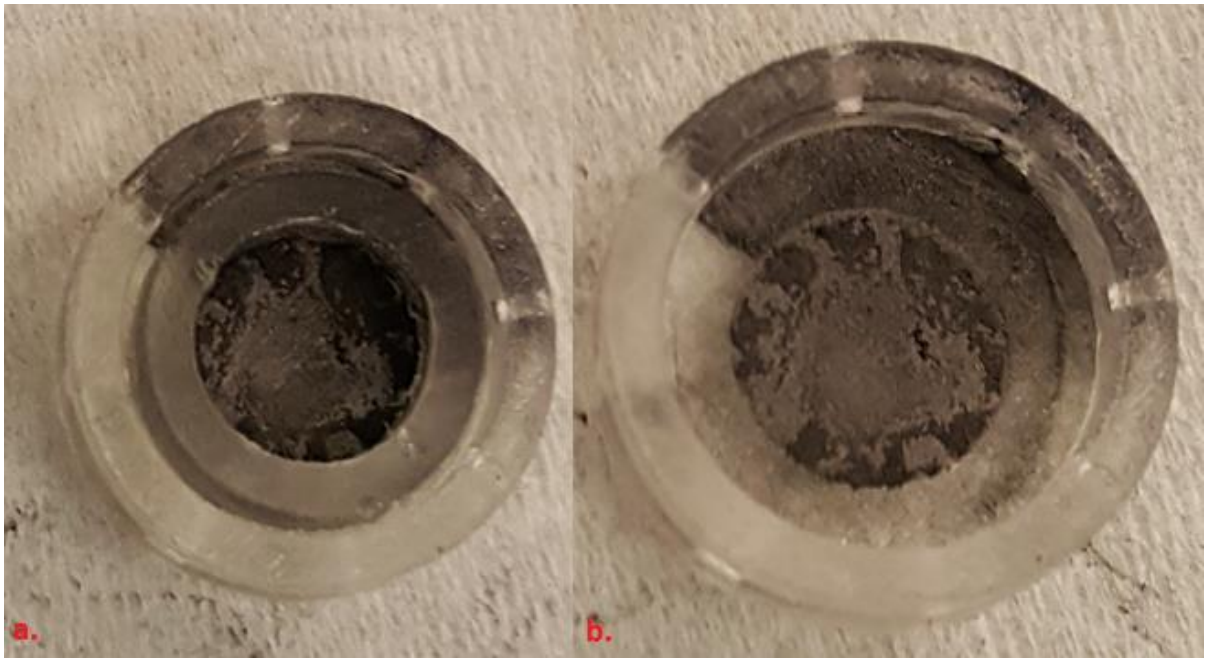

Figure 1a: Evaporated graphene solution droplets on rigid substrate cap with the mold in place. **b:** graphene on substrate after removal of the mold.

Instead two other methods were attempted to produce high quality graphene patterns from the prepared solutions. The first method utilizes a technique detailed by Oren et al [8]. A silicon wafer substrate is heated on a hotplate at 90 °C for five minutes. Then SU-8 photoresist is applied to the silicon wafer and spun at 500 rotations per minute (rpm) for 6 seconds. It is then immediately spun for another 25 seconds at 1500 rpm. Once the wafer has stopped spinning, it is baked in an oven for three minutes at 80 °C followed by 20 minutes at

100 °C. After the prebake is complete, the wafer is then covered by a printed photomask that exposes only the device pattern to the ultraviolet light. The UV exposure time is 75 seconds and has a light intensity of 8 milliwatts per square centimeter. When the exposure time is over, the wafer is heated on a hotplate at 90 °C for 5 minutes to post bake it, after which it is placed gently in SU-8 developer solution. The development process takes approximately 5 minutes, but the time can vary depending on the UV exposure process. As a result, isopropanol is applied to the edge of the wafer every 30 seconds after an initial 2 minutes of development. This creates white reagents while SU-8 is still present on the wafer surface. Once the reagents have noticeably decreased in concentration, the wafer is rinsed in acetone and deionized water and removed from the developing solution so as to not overdevelop the pattern created by the photolithography. Now a PDMS mold is created by first mixing PDMS elastomer and curing agent in a 10:1 ratio. After thoroughly mixing, the PDMS is placed in a degasser until no air bubbles remain. This takes approximately 30 minutes. Once the degassing is complete, the patterned wafer is placed into a petri dish, covered with the PDMS mixture, and heated at 85 °C until it has completely cured, after which the PDMS is removed from the petri dish and is ready for graphene deposition [8].

The ethanol-based graphene solution is dropped on top of the PDMS mold using a fine tip needle so that the layer is thin enough for quick evaporation. This evaporation process is done on a hotplate set to 85 °C and takes approximately 15 minutes. Once the solution has evaporated and only dry graphene remains on the surface the excess graphene around the mold is removed by applying polypropylene tape with very light pressure and peeling it away [8]. This process is repeated until only the graphene within in the mold remains. The graphene deposition process and the removal of excess is repeated until the

mold holds enough graphene sheets to meet the desired resistance value. For these sensors, this meant typically four or five cycles in order to achieve graphene resistance below 20 kilohms. After the final cycle is finished, polyimide tape is applied to the surface and firmly pressed into the mold so that the tape makes direct contact with the patterned graphene. When the tape is removed, the patterned graphene is peeled with it and is then placed in a furnace for 3 hours at 250 °C [8].

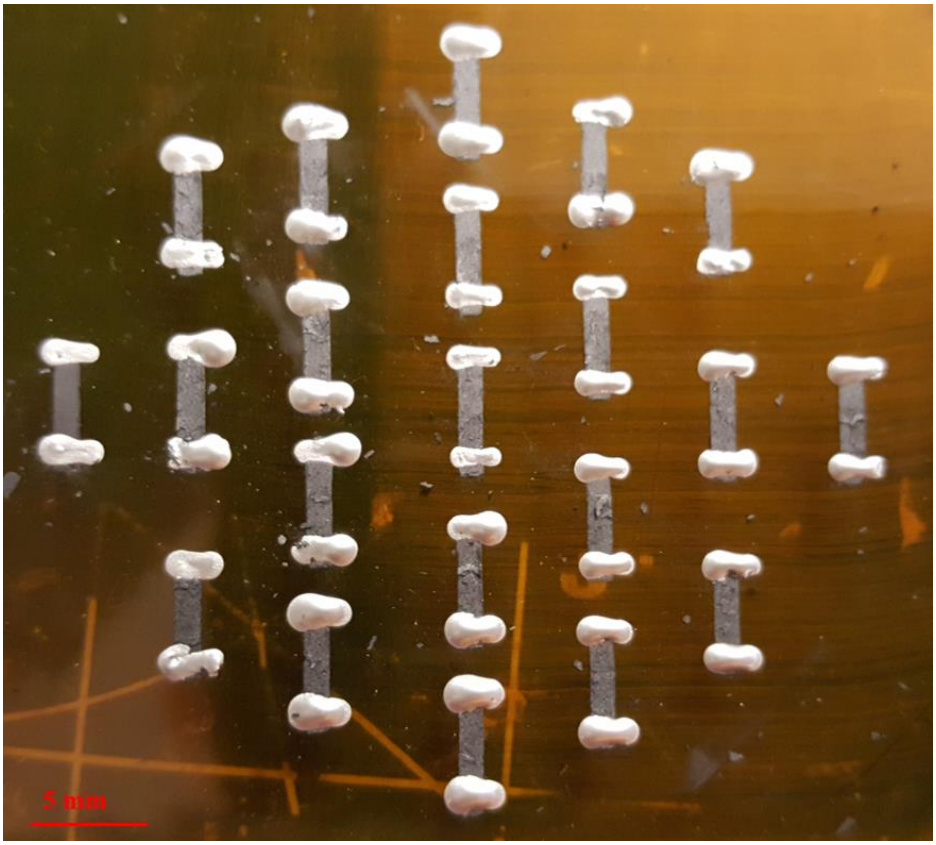

Figure 2: Graphene sensors fabricated using the PDMS mold after annealing and dispensing of silver paste.

The second attempted method of depositing graphene was inkjet printing. This was done using a Fujifilm Dimatix 2850 printer. Initially there were significant issues with attempting to print graphene solution using this system due to the jetting channels becoming blocked. It was later determined that the cause of the blockages was the result of the ethanol-based solution evaporating too quickly as it was printed. At this point, the water-only

graphene solution was prepared and used for the inkjet printer. This water-based solution indicated an improvement in the jetting process, but the relatively high surface tension of the liquid appeared to create a new issue. As the sensors were printed, the graphene ink would condense into larger islands on the polyimide adhesive surface, which resulted in a patchy pattern. To fix the new issue, acetone was added to the solution in a 3:1 water to acetone ratio. This improved the printing process, but in the end the devices still did not have electrical conductivity resulting in the use of just the molded graphene.

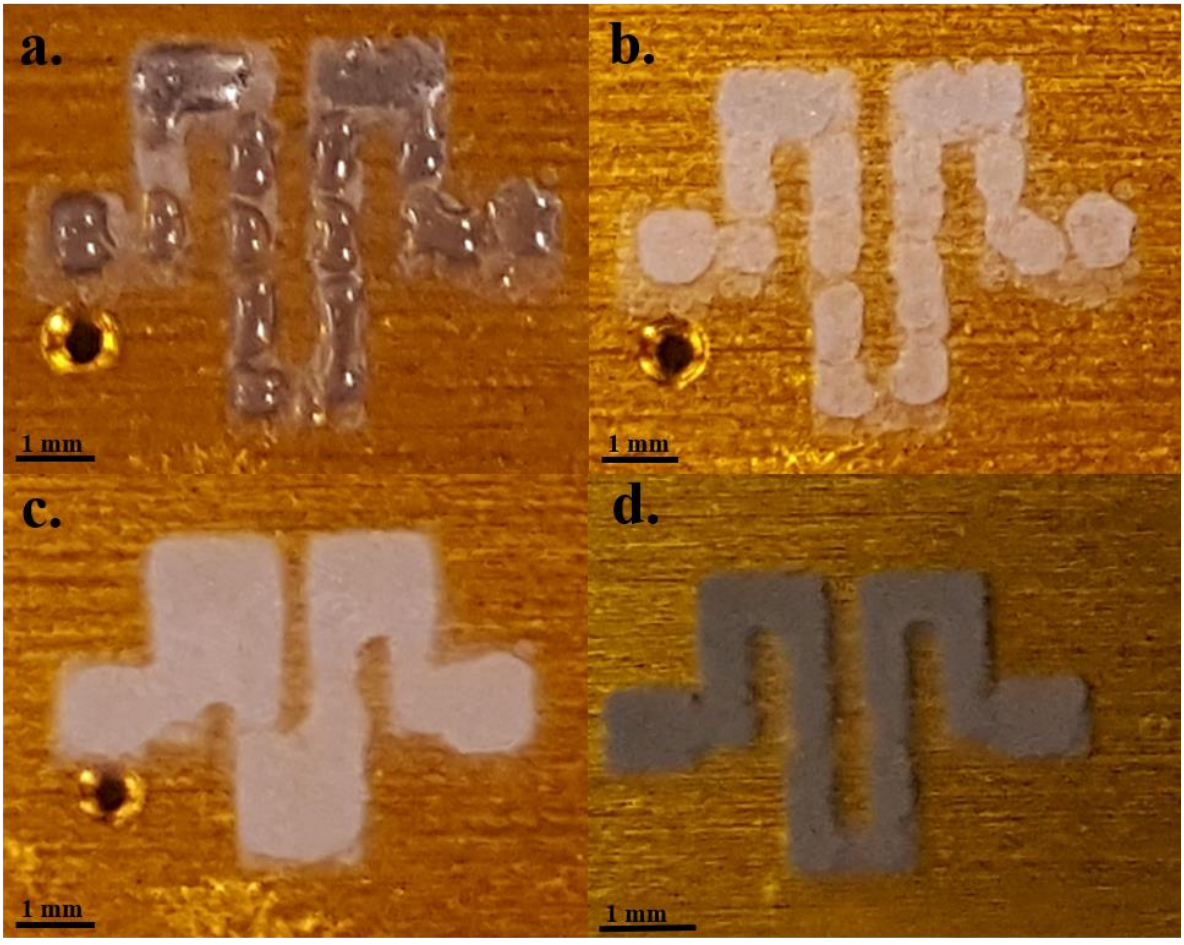

Figure 3a-d: Images of inkjet printed graphene sensors using different solutions and configuration settings. **a:** Second layer of printed graphene and deionized (DI) water solution with 10 um drop spacing in the process of evaporating. **b:** Post evaporation of the second layer of printed graphene and DI water. **c:** After the evaporation of the fifth layer of printed graphene and DI water solution with 5 um drop spacing. **d:** After the evaporation of the fifth layer of printed graphene dispersed in acetone and DI water solution using 5 um drop spacing.

Pattern Design

In general, the graphene sensors only need to create a stable electrically conductive path. For proof of concept tests, it is sufficient to utilize a simple rectangular pattern measuring 1.5 mm by 7 mm. The overall size is based on the need for covering a large enough area of stomata without being too cumbersome or heavy for the plant leaf. However, since the sensors are used to measure moisture content in the nearby air, a larger surface area is beneficial for sensitivity. In order to increase the surface area of the graphene pattern without disrupting air flow and without drastically increasing the size of the device, a zig-zag pattern is used for later tests (figure 4).

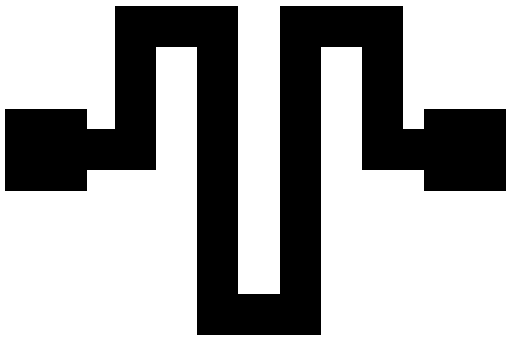

Figure 4: Graphene pattern produced in Photoshop for inkjet printing.

Electrical Contacts

The electrical contacts of the devices are comprised of two parts, silver chloride paste and gold coated spring pins. Once the graphene sensing component is annealed, silver chloride paste is deposited via a Nordson E2 EFD dispensing unit. The ideal method of deposition is to create a short rectangular style strip of the paste since any form of drop creates too much of a rounded dome shape. For this application, the machine pressure is set to 4 pounds per square inch (psi) with a needle movement speed of 0.2 mm per second. A

drop is initially placed next to one end of the graphene sensor and the needle then makes a forward and backward motion across the edge of graphene. This motion assists in evenly depositing and spreading the silver chloride paste into a relatively flat strip that is ideal for pin connections. After dispensing the paste, the sensor is annealed for another 3 hours at 125 °C. Silver chloride is used as opposed to pure silver as it is a more cost effective material and there is little loss in performance. For reference, a 1 millimeter by 1 centimeter strip of silver chloride paste was deposited on polyimide and annealed under the above conditions and resulted in a total end-to-end resistance of 0.8 ohms. Since the devices are operating in the 1-100 kOhm range, this additional contact resistance was deemed sufficiently irrelevant.

The second part of the electrical contacts is the gold coated spring pins. Two spring loaded pins (Mill-Max Manufacturing Corp. part 0900-1-15-20-75-14-11-0) are placed in the cap structure of the central device. The device is designed to twist into its final position wherein the pins are then aligned with and lightly compressed onto the silver chloride paste of the sensing component. This allows for wired or wireless connections to be made to the top of the pins without having to alter the design or manufacturing of the sensing graphene. In addition, the pins and cap structure are then removable and reusable for other devices.

Central Device Structure

Solid Vs. Flexible Structure

While a flexible device is attractive for adaptability in many cases, it can also be a detriment. For housing a graphene-based sensor, a flexible structure has the potential to cause issues in the quality of measurement. This could be anything from long term signal drift to the breaking of the electrical connection. These issues are possible because the graphene is

able to flex as the sensor flexes and stretches, which results in the graphene structure fracturing.

One way to combat this issue is to attach the graphene sensing component to a solid substrate instead. As the leaf grows, the main device structure is unaffected, meaning the graphene is better able to maintain a base resistance level. The main drawback of using a solid structure is that it is less adaptable to changes in the surface it is attached to, which in plant applications is a concern. To alleviate strain on the plant leaf, a flexible polymer is used as an intermediate structure between the main sensing device and the attachments on the leaf.

Structure Design

The central device structure is based on a twist cap design (figure 5). The lower half is similar to a shallow open topped cylinder in which the graphene is placed on the bottom surface. Two L-shaped grooves are cut into the inner sides of the cylinder and serve as the channels for the top piece to slide and twist within. There is also an expanded ring around the outside for attaching the flexible polymer. The top half of the device has two small knobs that stick out on either side that slide down into the cylinder's inner channels. While sliding downward, the cap is then able to twist sideways 90 degrees into its final resting place. To maintain contact between the top cap and the graphene residing on the bottom surface, gold coated spring pins are connected into the cap. When the cap is rotated the designed 90 degrees, the two pins are aligned with the silver chloride paste on top of the graphene sensor.

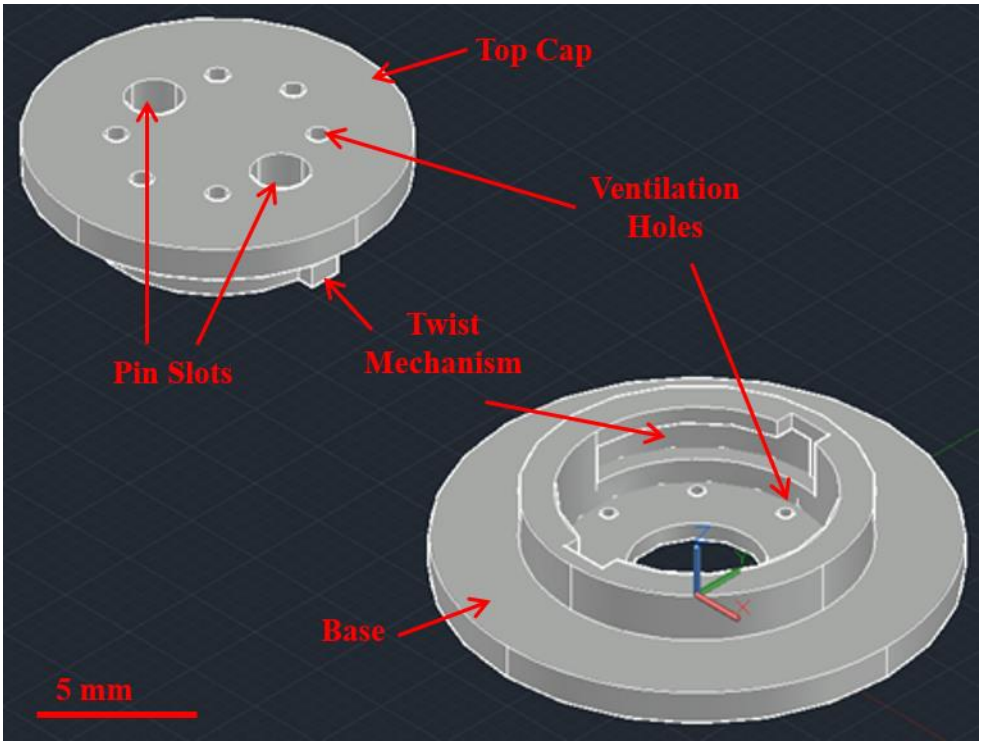

Figure 5: AutoCAD design of central substrate which includes a twist connection system, airflow holes, and electrical contact pin locations.

Initially, other cap connection designs were explored. The first was a snap-based connection that would keep the two pieces locked together with the goal of improving stability, but this also meant that the device could not be reopened, limiting its reusability. Another method was screw threading to twist the cap into place. This method is more ideal than the simpler press and twist style of the final design, but was difficult to fabricate using 3D printing. The final design is an adequate comprise that allows for reusability, part replacement, and is fairly stable when closed.

3-Dimensional Printing of Device

The two device portions are designed in AutoCAD and then converted into a file type recognized by the formlabs printer. The 3D printer uses a mixture of methacrylic acid esters and a photoinitiator to produce the designed pieces. After the printing is finished, the devices are rinsed in isopropyl alcohol for five minutes to wash away the extra material resin. Then

they are dried in room temperature. If the printed devices are still slightly soft, they are left exposed to radiant light to help form cross links in the material.

Flexible Leaf Attachment

Inhibition of Leaf Growth

An issue with measuring various characteristics of living organisms during their life cycle is that they are not reserved to a single set of conditions. For corn plants basic properties such as height, leaf length, and leaf width continue to change over time. In addition, more complex properties like moisture uptake also change as naturally a decaying plant is no longer absorbing water. This means that there are many variables in action that are either deemed irrelevant or require some form of compensation. The goal of this sensor is to maintain the ability to monitor moisture content of the plant while not inhibiting growth.

A rigid device fixed at multiple points to the underside of a corn plant leaf, will fundamentally not allow the leaf in that region to grow in a natural manner. This inherently puts stress on the leaf in the sensing area. Also, the quality of the signal is affected if the attachment points are too close to the sensing area due to blocking of stomata and leaf decay. By using a soft polymer as a flexible attachment structure, the leaf is able to grow more naturally and allows for separation of the binding and sensing regions.

Design of Flexible Component

Initially, there were numerous styles of design for the flexible attachment component. One such design included individual waved bars with a 2 millimeter by 5 millimeter footprint that would bind to two different ends of a solid device. While simplistic, the small size was difficult to handle and made any method of device assembly inconsistent. Another concept involved creating a ring-like structure, similar to a rubber o-ring that created a

conformational buffer between the solid device and the plant. This was easier to assemble and incorporate into the device, but would have less range for axial expansion.

The original design is a combination of the previous ideas. There is a ring-like structure that surrounds the base of the rigid device, which has four evenly spaced arms that spread outward (figures 6,7). These arms have a sinusoidal wave pattern that, when compared to a straight structure, alleviates stress when stretched. Eventually it was determined that the device did not require as large a range of flexibility as originally anticipated, so tests were also done using just a ring structure without the arms.

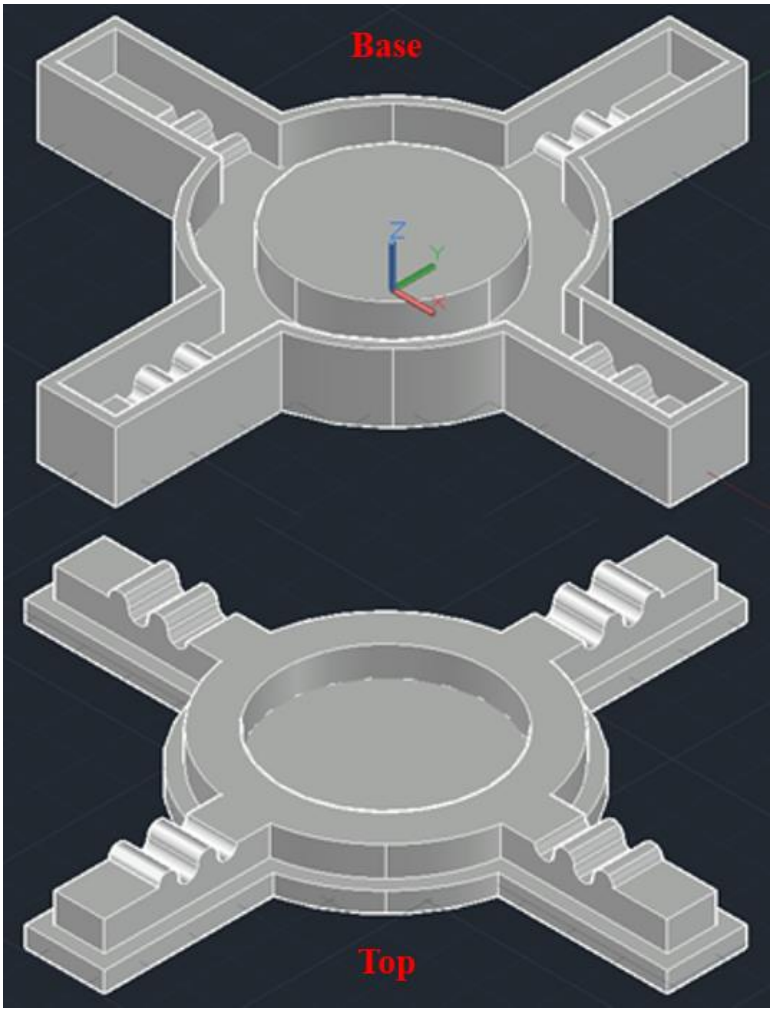

Figure 6: AutoCAD design of the mold used to produce the ecoflex attachments.

Fabrication of Molded EcoFlex

The soft polymer is created by first mixing Smooth-On's Ecoflex 00-30 part A and part B at a 1:1 ratio. Then degas the mixture for 45 minutes to remove any air bubbles. After the polymer is thoroughly degassed, it is syringed into the bottom half of the 3D printed mold until it is completely filled. The top portion of the mold is then placed onto the base and pressed down firmly creating a seal. Once the molds are closed, they are placed on a hotplate and cured at 70 °C for 30 minutes. At this time the molds are opened and the cured polymer is carefully removed using tweezers.

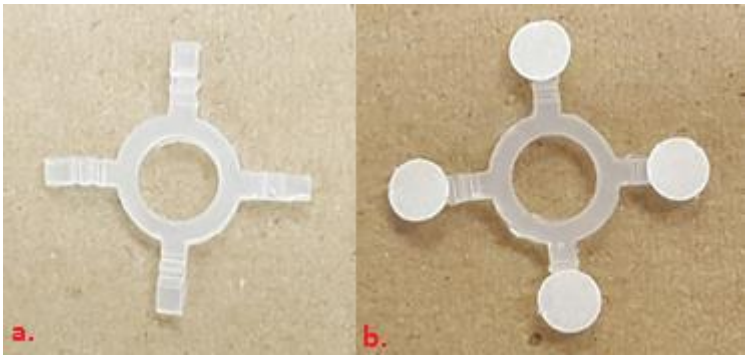

Figure 7a: Fabricated ecoflex produced from the 3D printed mold. **b:** the ecoflex with the adhesive pads attached to the end points.

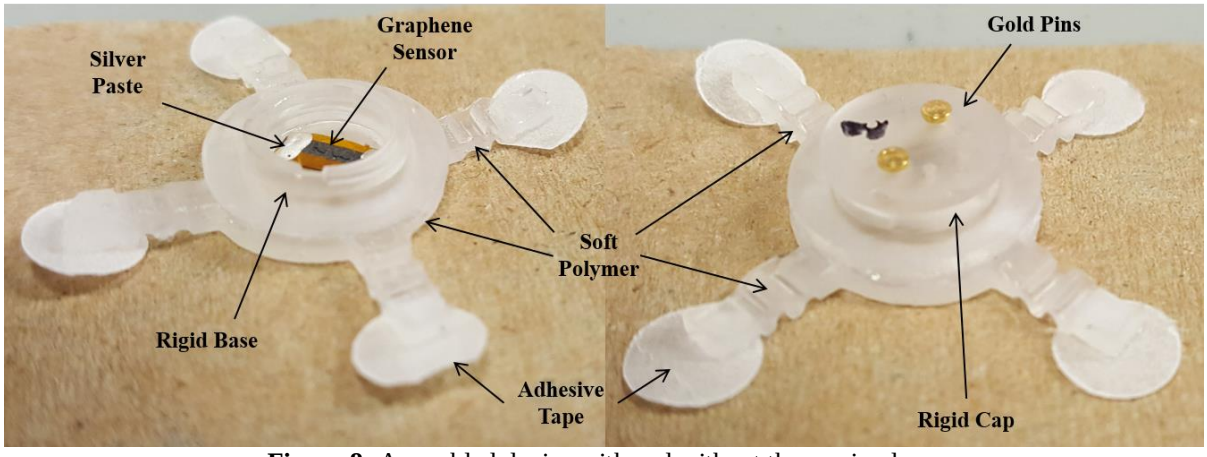

Figure 8: Assembled device with and without the cap in place.

CHAPTER 4. RESULTS AND DISCUSSION

Mechanical Analysis

Dynamic Material Analysis

Mechanical simulations are performed to test the efficacy of the basic design, but in order to do so, tests are required to determine the true material properties. Two ratio variations of the silicone rubber, 2:1 and 1:1, are prepared using the method described previously. The two combinations are then poured into plastic petri dishes and cured under various temperatures and lengths of time. After curing, the polymers are cut into 12 mm by 40 mm samples for dynamic material analysis.

Static stress tests are conducted on each of the samples using a TA Instruments RSA-G2 Solids Analyzer. The stress is measured while slowly applying 100 mm of strain at a rate of 1 mm per second. From the stress-strain data, it is found that the material properties are not dependent on dimension, which is expected. In general though, there is a small difference in mechanical response of the samples, with the 2:1 ratio polymer having a slightly higher stress (figure 10).

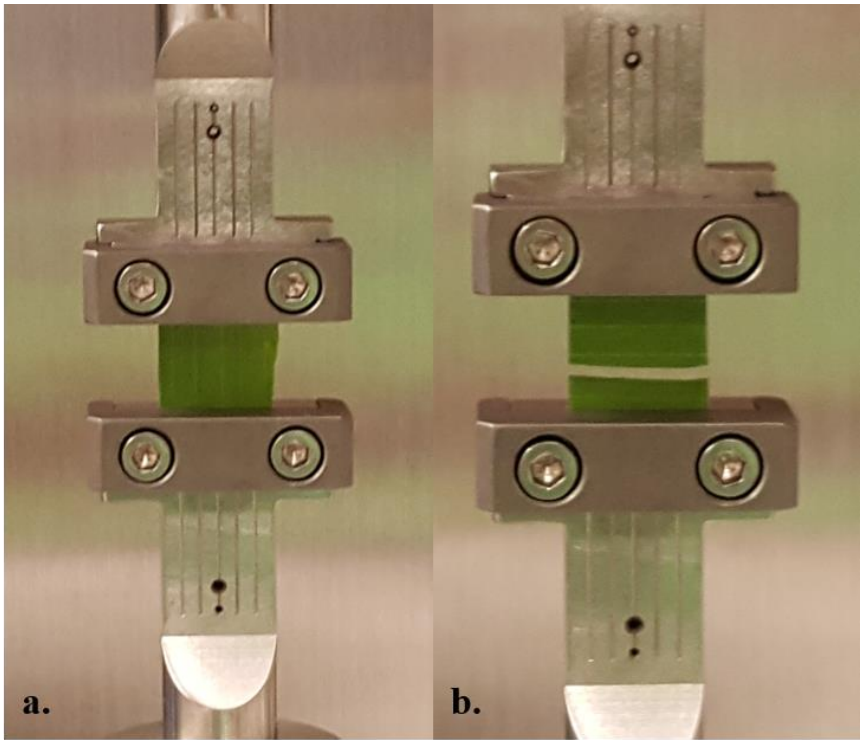

Figure 9: Corn leaf samples undergoing static stress test using a TA Instruments RSA-G2 Solids Analyzer. **a:** Strain applied in the axial direction during testing. **b:** Aftermath of the leaf when strain is applied in the transverse direction.

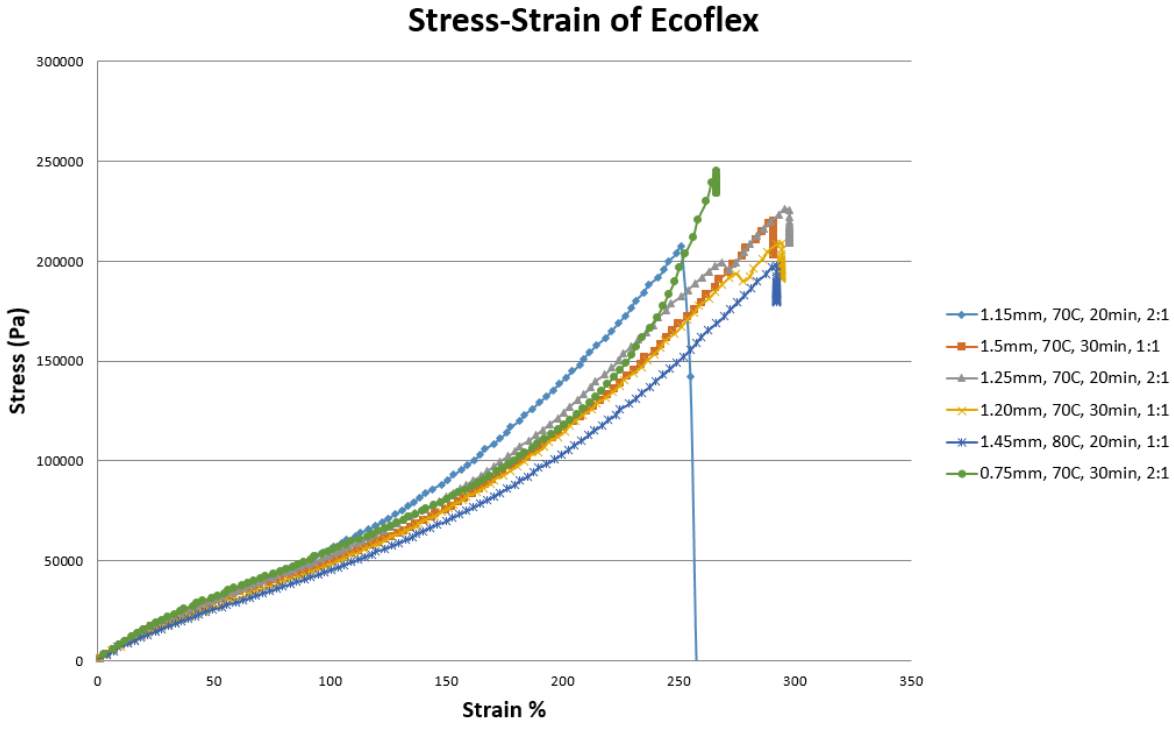

Figure 10: Stress-strain results of various ecoflex samples.

Based on the measured dimensions and the stress-strain data, the dynamic material analyzer computes the Young's modulus. This data follows a similar trend in that the general response is similar with the 2:1 polymer samples have a slightly higher modulus. Overall the modulus ranges from about 45,000 to 60,000 Pascals for the expected levels of strain (figure 11).

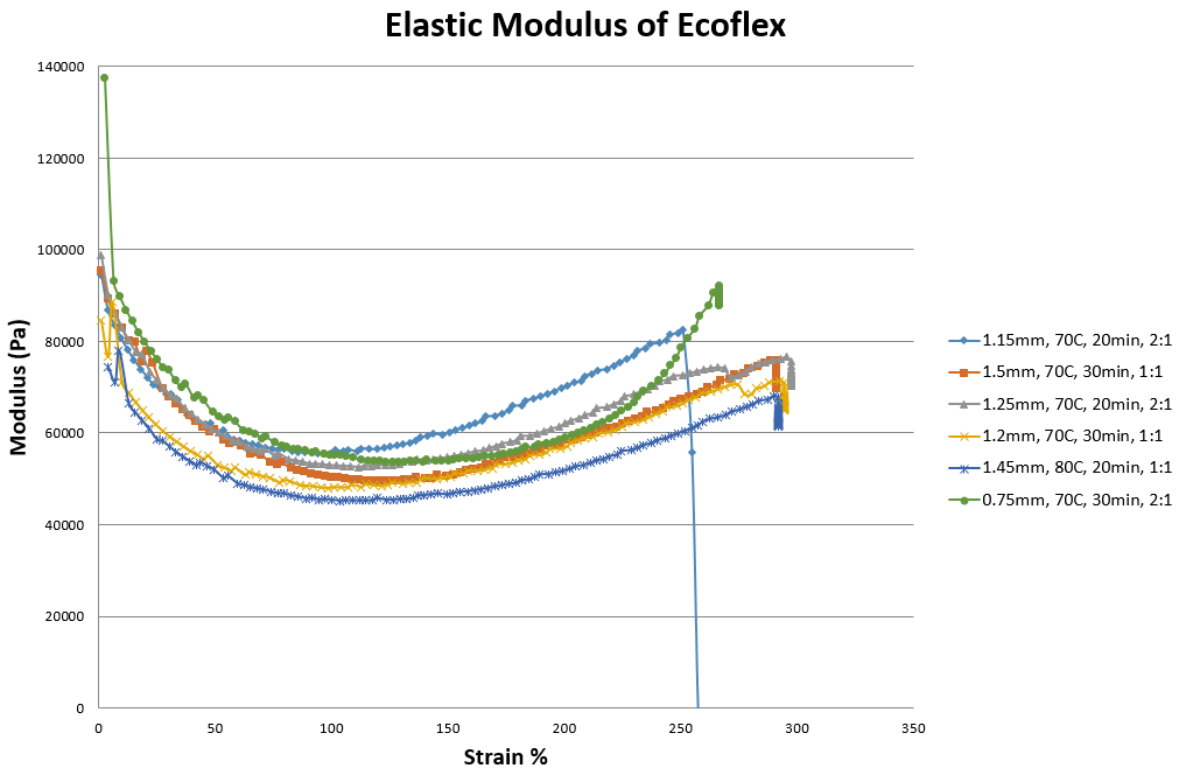

Figure 11: Elastic modulus of the ecoflex samples as calculated by the dynamic material analyzer during the static stress test.

In addition to analyzing the soft polymer material, dynamic material analysis was also performed on samples of corn plant leaves. Four samples with a cross section of 12.5 by 11 mm and thickness 0.2 mm were strained at a rate of 0.01 mm per second. Two of the samples were placed so that the strain was applied parallel to the plant fibers and the others with it perpendicular. Since plant leaves are anisotropic due to their physical structure, the expectation is that their modulus will also greatly depend upon the direction of applied strain.

Specifically, the expectation is that the plant will be weaker in the direction perpendicular to the fibers. After performing the analysis, it is apparent that this is the case as the samples strained along the fiber axis had a Young's modulus of about 65 MPa and the ones strained perpendicular to the fiber had a modulus of just under 20 MPa. There are a few things to note with this testing process. One is that it is difficult to measure the stress-strain response of the plant leaves as the clamps holding the ends down can slip since plant matter compresses easily. Secondly, the tests performed against the fiber direction can vary more as any small fracture in the leaf quickly propagates along the fiber length, resulting in a complete tear that can occur at different levels of strain for each sample.

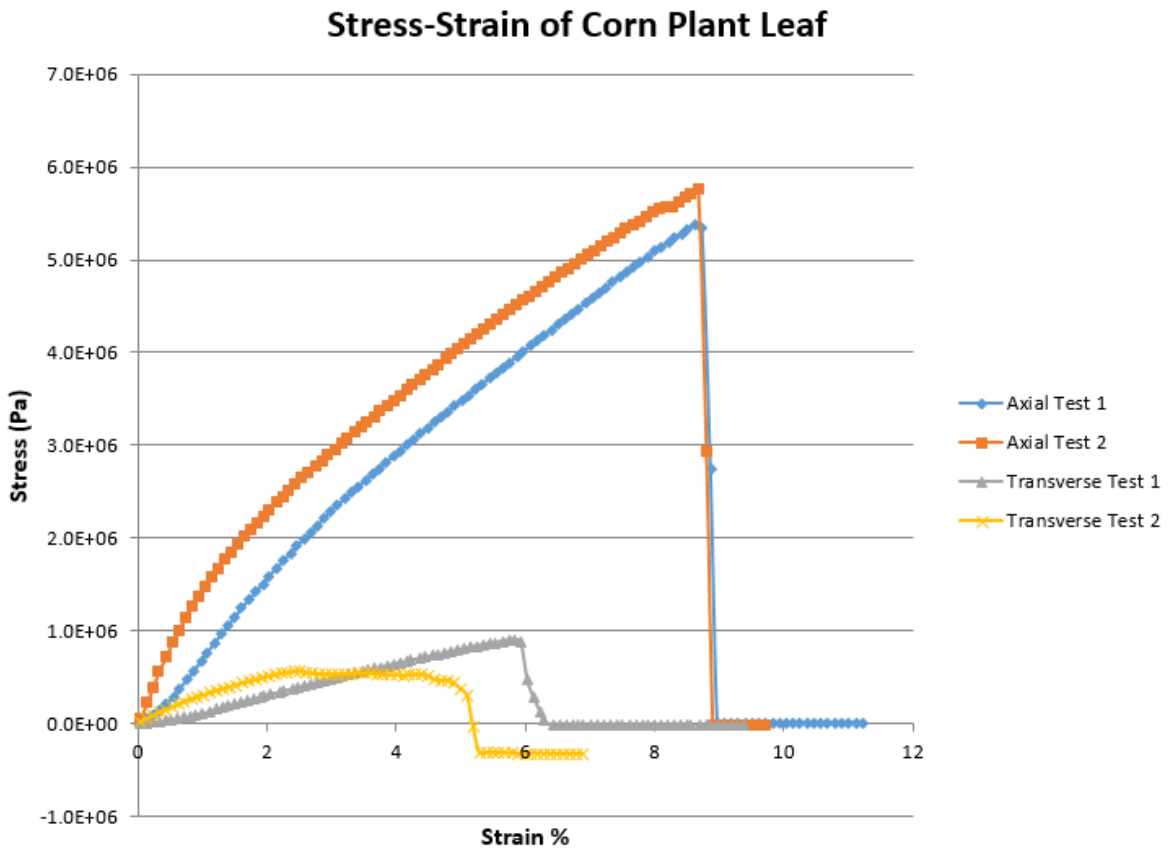

Figure 12: Stress-strain relationship of corn leaf samples with strain applied in both the axial and transverse directions.

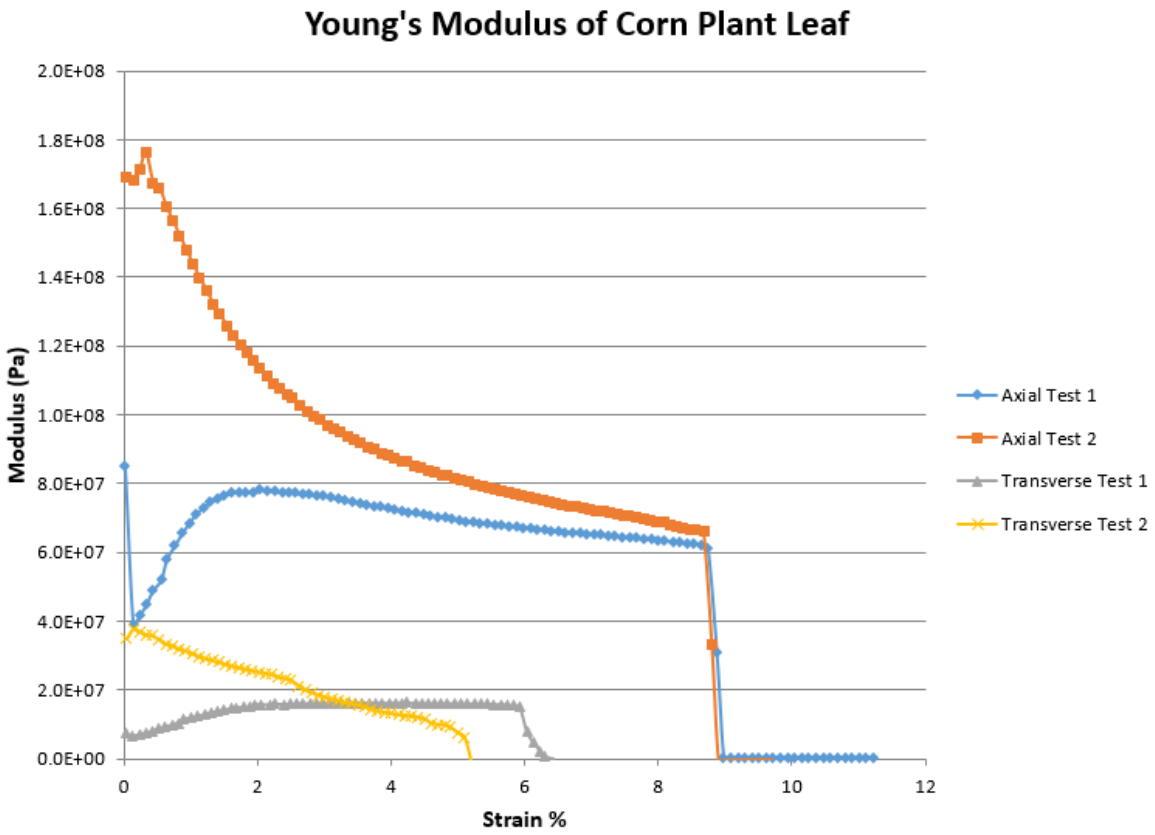

Figure 13: Young's modulus of the corn leaf samples as calculated by the dynamic material analyzer during the static stress test.

Mechanical Simulations

Two mechanical simulations are performed using COMSOL software and the previously found modulus values with the goal of determining the effects of the soft polymer structure when bound to the plant leaf. The first simulation models the straight polymer arm and the second models the sinusoidal structure version. Figures 14 and 15 display the stress profile of the devices after applying a force of 1000 newtons to the end of the flat leaf structure. This stress profile is similar for both, but the values are slightly lower across the whole structure in the sinusoidal device indicating that it is the better structure for alleviating stress on the system. Also, these simulations show that the sinusoidal structure provides less resistance on the leaf and is able to expand more under the same amount of applied force.

One side thing to note is that the system does not appear to have a gradual stress gradient across the material interfaces, but this is due to the drastic differences in material properties. When modeled all as one material, the system does have a more gradual gradient near all corners and edges while also demonstrating the enhanced flexibility of the wrinkle structure and its impact on the integrity of the system.

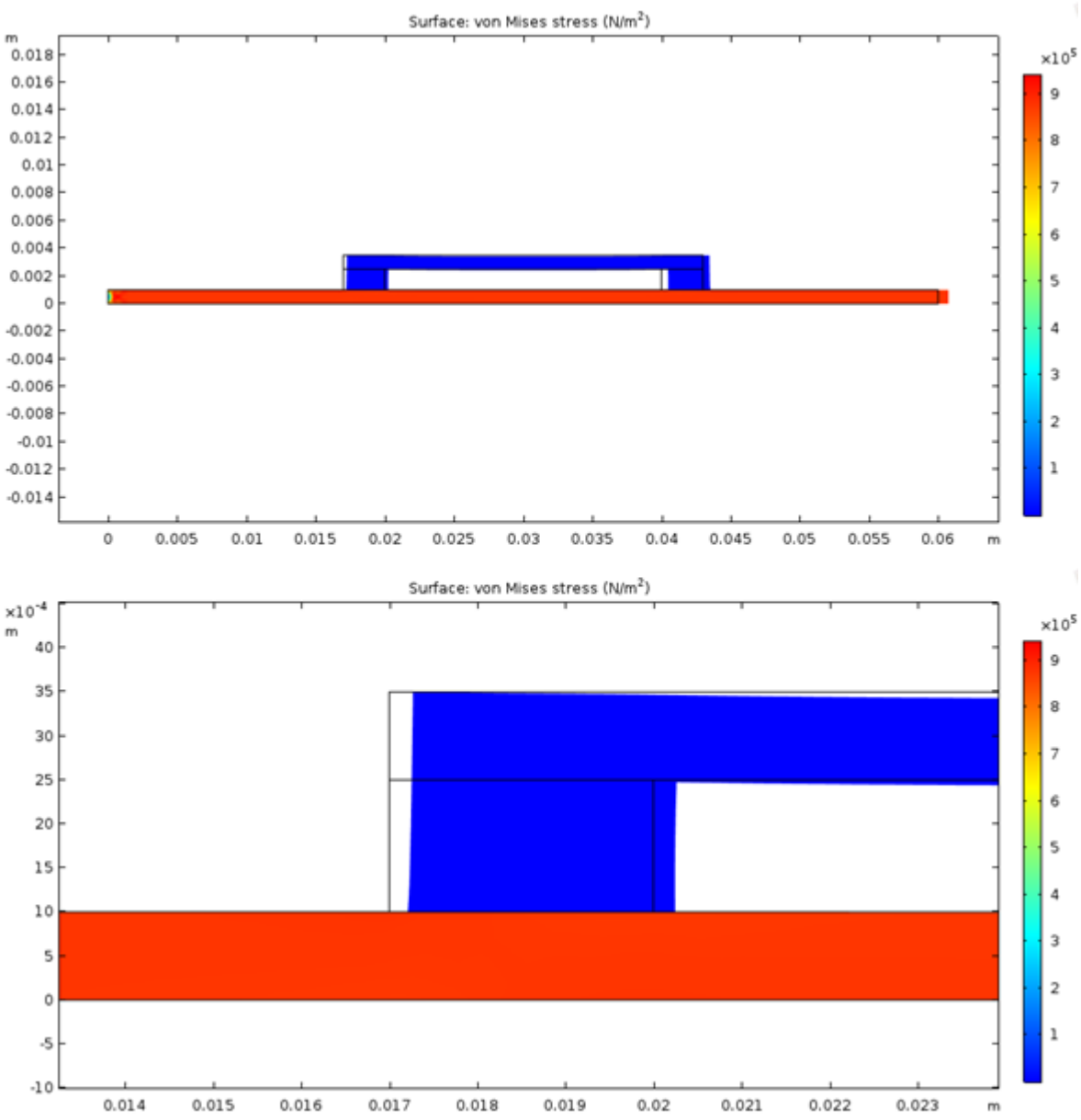

Figure 14: COMSOL simulation of straight ecoflex arm attachments bound to plant leaf undergoing high applied stress.

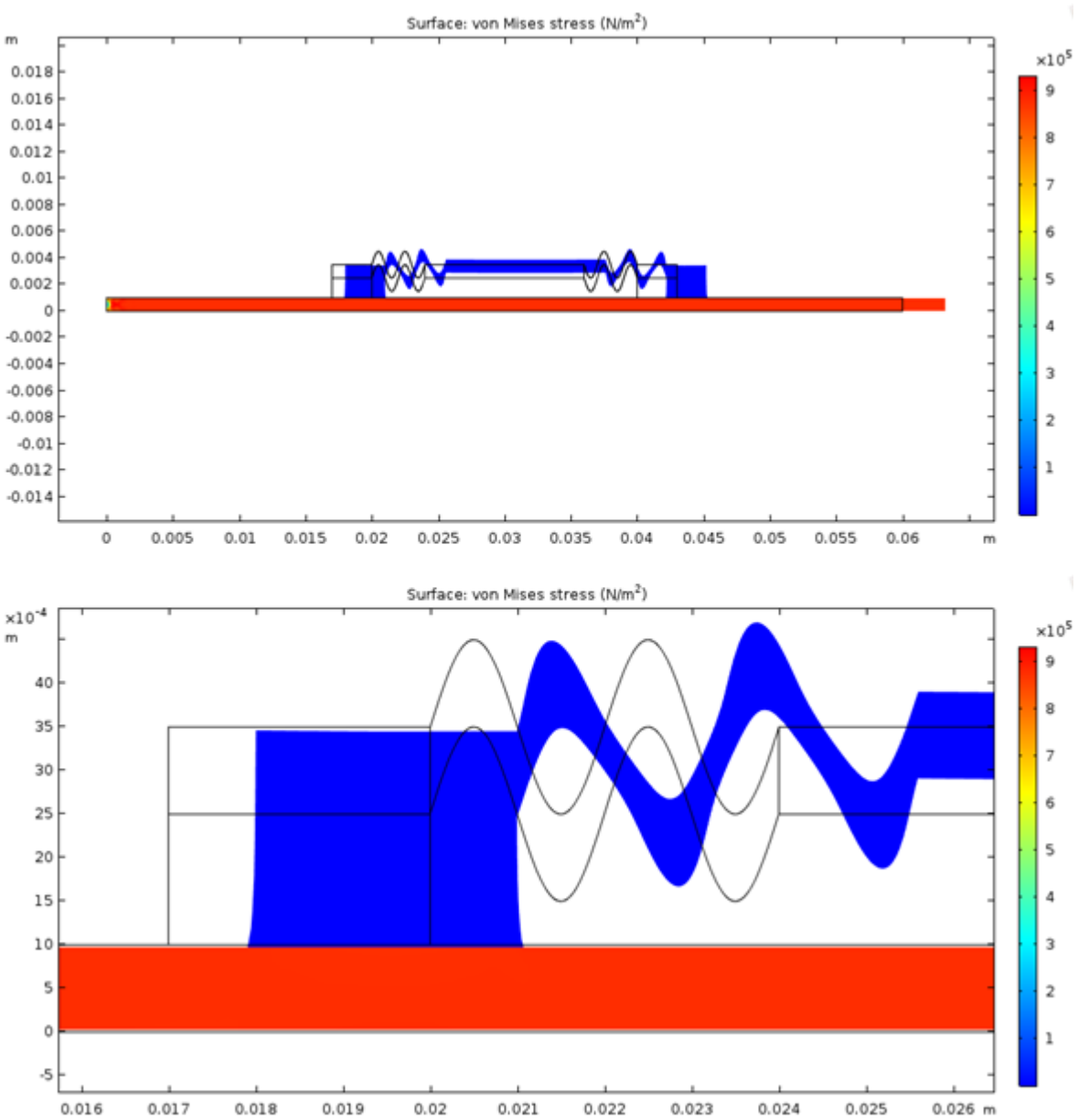

Figure 15: COMSOL simulation of wrinkled ecoflex arm attachments bound to plant leaf undergoing high applied stress.

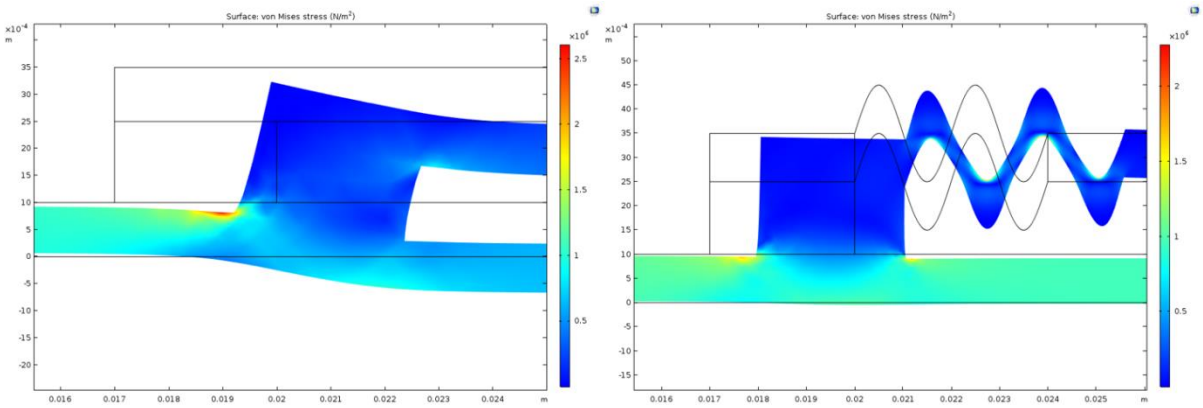

Figure 16: COMSOL simulation of straight bar and wrinkled ecoflex arm attachments bound to plant leaf undergoing high applied stress, but using only the leaf material properties for every component.

In-situ Image Analysis

The original expectation of plant growth was that the plant leaf would expand in addition to changes in curvature and shape. However, after various studies, it is found that the most predominant growth is done at the base of the plant leaf resulting in the sensor undergoing more translation movement away from the stem as opposed to extensive stretching. Based on images taken throughout the testing cycle, there is some indication of device stretching and twisting, but not enough to conclude that the flexible arm structures are necessary for stable signal measurement (figure 17).

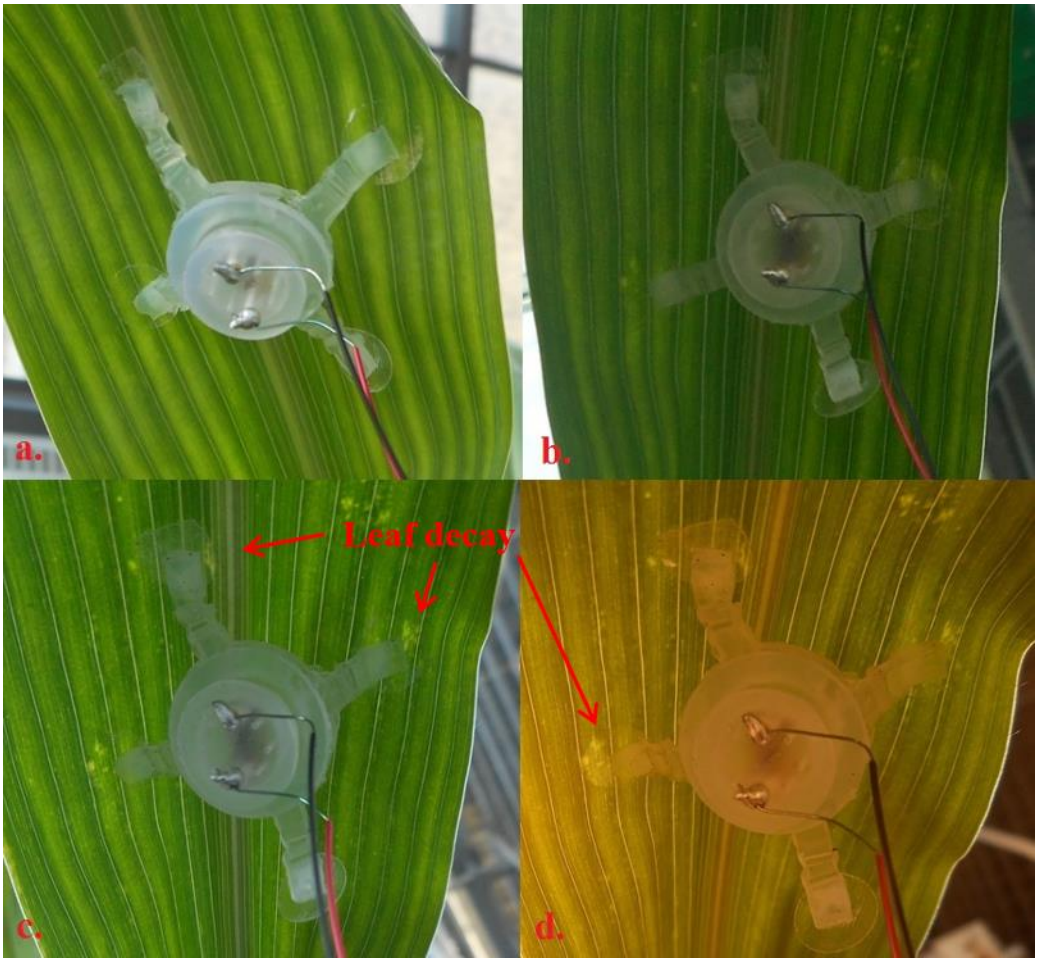

Figure 17a-d: Images of the sensor during testing period on days 1, 8, 13, 14 respectively.

Moisture Sensing Capability

When making mechanical changes to a sensor device, it is important to make sure that those changes do not hinder the sensor's ability to perform its intended function. In the case of moisture sensing of plant leaves, the graphene sensor is best able to interact with the water molecules when it is close to the stomata, but not blocking them. If the sensor is too far the leaf, then the resulting signal will predominantly be measuring the environmental conditions, and not the plant contributions. For reference, the previous work done by Oren et al. has the sensor approximately 100-200 micrometers from the leaf surface, whereas this new design places the sensor at about 4 millimeters away.

To test the performance of the graphene sensor a five-day study was performed in a greenhouse. Wires were soldered onto the gold pins of the twist cap and the sensors placed on the underside of corn leaves near the stem. The data was measured using NeuLog resistance data loggers, which recorded a value every thirty seconds. During this trial, two other sensors were attached to a non-biological surface in order to measure just the effects of the room temperature and humidity. However, those sensors were only active for the first three days due to loss of battery power. Based on the results, it is clear that the sensors indicate the change in the greenhouse temperature and humidity, with the temperature creating a stronger response. The humidity response is harder to analyze, but there is some form of inverse relationship between the environmental humidity and the sensor data.

The data however does not clearly indicate plant transpiration. Comparing the control and plant sensors, there is some correlation, which is especially noticeable during the midday increase in resistance, but it is difficult to make any conclusion whether the differences in the plant sensor are truly a result of the plant contribution. With this in mind, another trial was performed with both the biological sensor and the control sensor being attached to the underside of the leaf. The active moisture sensor was attached the same as before, but the control sensor was flipped so that the graphene was facing away from the leaf. The goal of this test was to create a better test versus control comparison by making the control be in the same locale as the test sensor. Essentially, by being in the same area and attached to the same portion of the leaf, both sensors would be under the same environmental conditions and physical conditions. Previously, the control sensors were located in another area of the greenhouse. The results of this experiment show that the two signals are very similar, indicating that the graphene sensor is primarily measuring the environmental conditions and

not plant transpiration. The likely reason for this is that the soft polymer arms, while good at not inhibiting the plant growth, are too soft to keep the sensor held closely to the leaf surface.

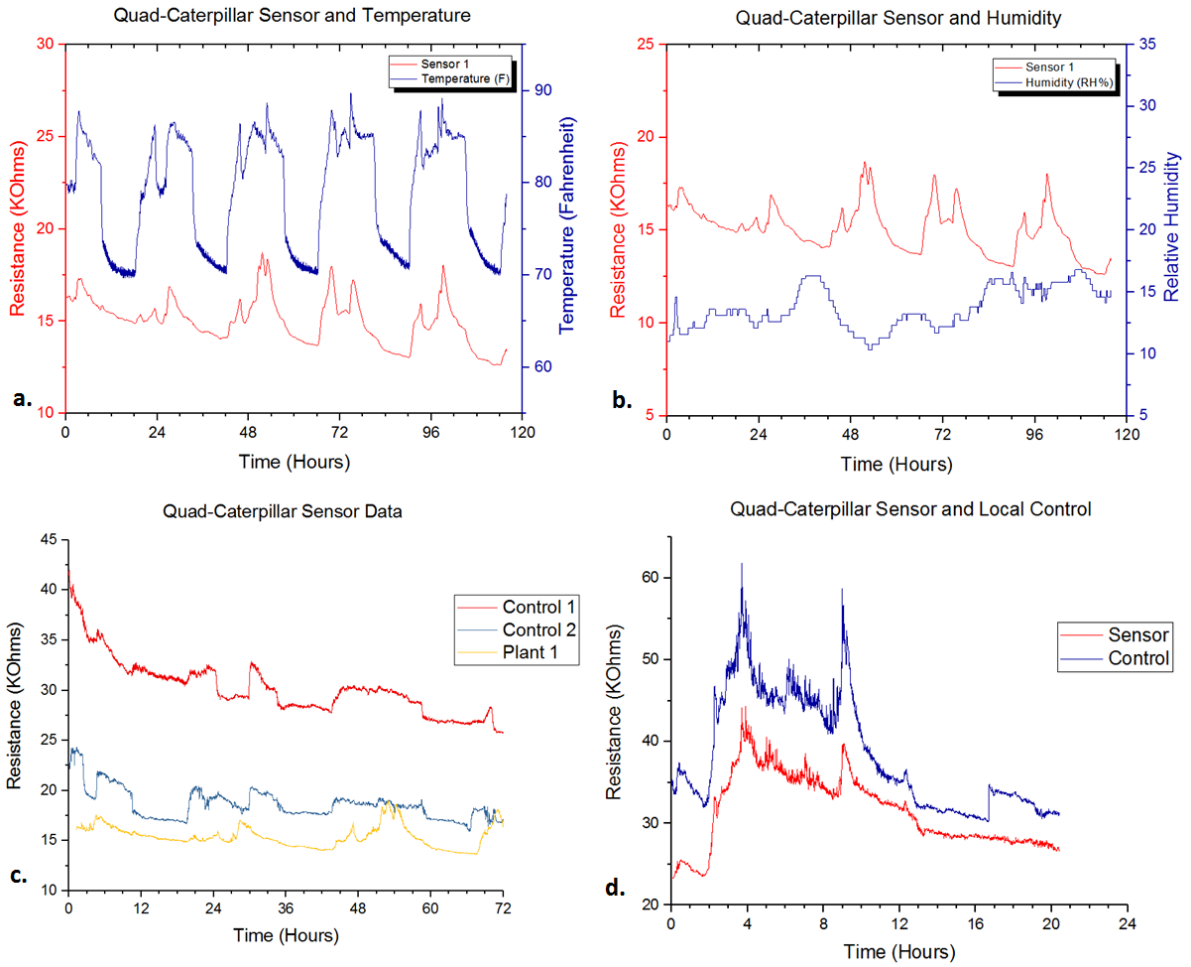

Figure 18a-d: Initial results of the moisture device. **a:** sensor data compared to environmental temperature. **b:** sensor data compared to environmental humidity. **c:** sensor data compared to control sensors in the greenhouse. **d:** sensor data compared to local control sensor placed together at leaf surface.

In order to remedy this, the soft polymer was changed to no longer include the extended arms. Instead, the adhesive is place at four points equidistant around the ring. The ecoflex is still there to provide conformational contact, but without the suspension mechanic the device does not hang away from the leaf at all, decreasing the gap between the leaf and the sensor to approximately one millimeter. With this design change, a new test was performed using sensors with and without the extended arms. Similar to the previous

experiment, one of each sensor were placed next to each other on the underside of a leaf so that a better comparison could be made.

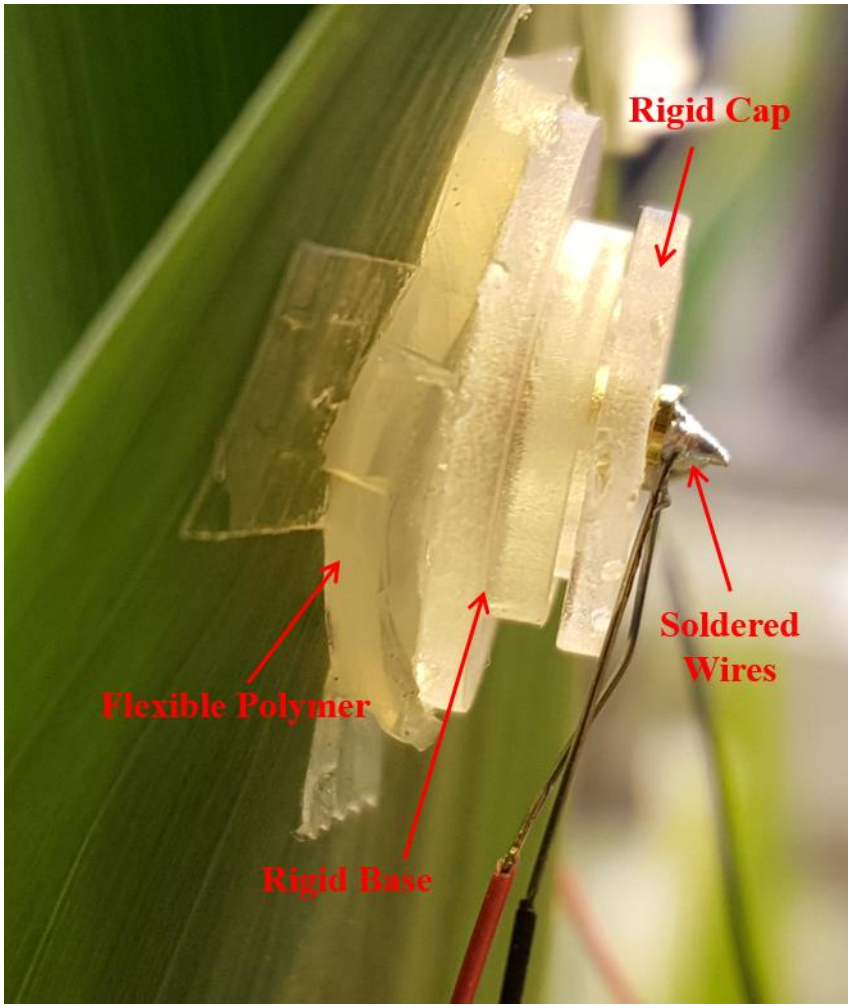

Figure 19: Quad-Caterpillar sensor design after removal of the four extended arms.

The first thing that is evident from this new study is that the armless sensor is much less stable than the one with the flexible extended arms. This could be a result of mechanical instability, but may also indicate better sensitivity to the leaf transpiration. For the previous design utilizing the quad-caterpillar attachment, the predominant contributor to the signal was the room temperature, which is typically a very stable condition. The armless sensor should also be responding to the greenhouse temperature, but other signal changes are expected if the design is better at detecting moisture content from the leaf itself. After taking

into account the point in time in which the plant was watered, it is evident that the new armless sensor is not able to detect the release of water vapor through the leaf stomata.

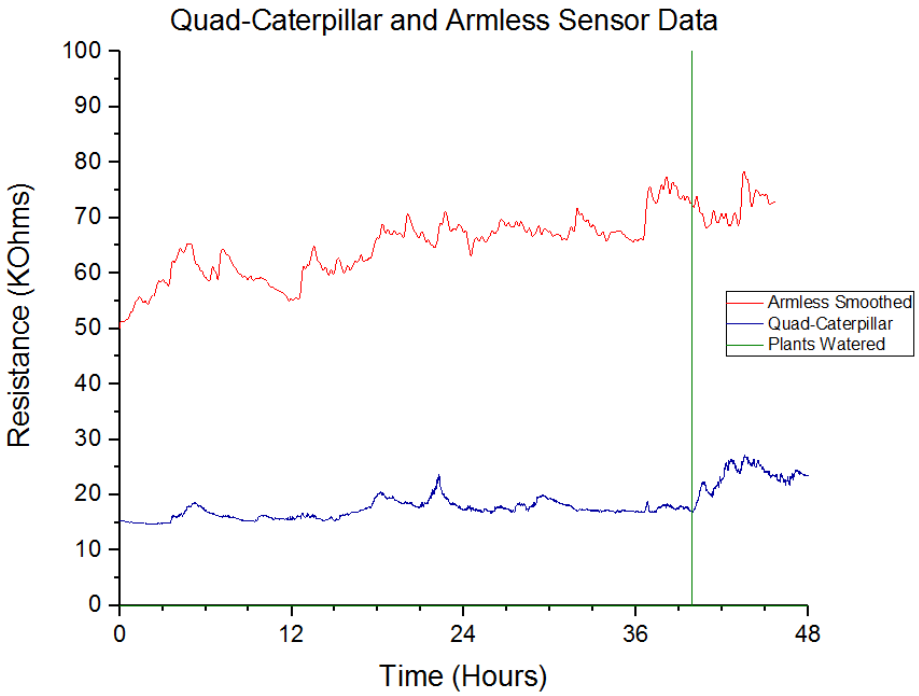

Figure 20: Comparison of quad-caterpillar design and a sensor with the winkled arms removed.

CHAPTER 5. CONCLUSION AND FUTURE WORK

The mechanical structure utilizing the soft polymer ecoflex along with a rigid central device is an interesting design that does alleviate some issues of previous devices. The graphene sensing component is more stable and less prone to fracturing. Also the use of compressed gold coated pins to make contact with the sensor allows for easier and more stable electrical connections. However, due to the nature of corn leaf growth, the flexible attachment can also be a hindrance when it allows the sensor to drift away from the leaf surface. Removing the extended arms while keeping the primary soft polymer ring maintains the conformational contact advantage while also holding the sensor as close to the leaf as possible. Lastly, the graphene sensor itself is likely too far from the stomata to be able to detect the expulsion of water vapor. Overall, it is determined that the extended arm structure of the soft polymer is unnecessary as the leaf primarily undergoes growth at its base, producing translational movement of the sensor instead of local expansion. The general mechanical design is also insufficient for measuring plant transpiration as the graphene sensing component is too far from the leaf surface.

There are a few adjustments to explore in future work that may improve the overall design. Firstly, changing the electrical connections to a wireless method will help reduce the weight and pull on the sensor and could potentially improve the signal quality. Also, utilizing inkjet printing for the production of the graphene sensors and silver contact coatings will improve fabrication throughput and consistency. This was something attempted in this work, but it was abandoned due to complications in the process. Lastly, any improvement in structural changes that bring the graphene closer to the place leaf surface will assist in detecting the portion of the signal that is a response to the plant transpiration. The farther the sensor is from the leaf, the more the response is dominated by environmental conditions.

ACKNOLEDGEMENT

The information, data, or work presented herein was funded in part by the National Science Foundation under the grant number DBI-1353819, the United State Department of Agriculture (USDA) under the grant number 2018-67021-27845, and the Plant Sciences Institute at Iowa State University.

REFERENCES

[1] T. Juenger, J. McKay, N. Hausmann, et al. “Identification and characterization of QTL underlying whole-plant physiology in Arabidopsis thaliana: δ13C, stomatal conductance and transpiration efficiency,” Plant, Cell and Environment, Vol. 28, Issue 6, Pgs. 697-708, (2005)

[2] W. Schlesinger, S. Jasechko, “Transpiration in the global water cycle,” Agricultural and Forest Meteorology, Vol. 189-190, Pgs. 115-117, (2014)

[3] L. Taiz, E. Zeiger, I.M. Moller, A. Murphy, “Plant Physiology and Development,” 6th edition, Sunderland, MA: Sinauer Associates, Inc. p. 101. (2015) ISBN 978-1-60535-255-8

[4] W. Cannon, “A New Method of Measuring the Transpiration of Plants in Place,” Bulletin of the Torrey Botanical Club, Vol. 32, No. 10, Oct. (1905), DOI: 10.2307/2478527

[5] R. Pearcy, E-D. Schulze, R. Zimmermann, “Measurement of transpiration and leaf conductance,” Plant Physiological Ecology, 137–160. (1989) doi:10.1007/978-94-009-2221-1_8

[6] S. Hunsmann, K. Wunderle, S. Wagner, U. Rascher, U. Schurr, V. Ebert, “Absolute, high resolution water transpiration rate measurements on single plant leaves via tunable diode laser absorption spectroscopy (TDLAS) at 1.37 μm,” Applied Physics B, 92: 393. (2008)

[7] X. Zhao, Y. Long, T. Yang, J. Li, and H. Zhu, “Simultaneous High Sensitivity Sensing of Temperature and Humidity with Graphene Woven Fabrics,” ACS Applied Materials & Interfaces 2017 9 (35), 30171-30176 DOI: 10.1021/acsami.7b09184

[8] S. Oren, H. Ceylan, P.S. Schnable, and L. Dong, "High-resolution patterning and transferring of graphene-based nanomaterials onto tape towards roll-to-roll production of tape-based wearable sensors," Advanced Materials Technologies, 2, 1700223 (2017)

[9] E. W. Hill, A. Vijayaragahvan and K. Novoselov, "Graphene Sensors," in IEEE Sensors Journal, vol. 11, no. 12, pp. 3161-3170, Dec. (2011), DOI: 10.1109/JSEN.2011.2167608

[10] Z. Li, L. Chen, S. Meng, L. Guo, J. Huang, Y. Liu, W. Wang, X. Chen, "Field and temperature dependence of intrinsic diamagnetism in graphene: Theory and experiment". Phys. Rev. B. 91 (9): 094429. (2015)

[11] K. Novoselov, A. Geim, S. Morozov, D. Jiang, Y. Zhang, S. Dubonos, I. Grigorieva, A. Firsov, "Electric Field Effect in Atomically Thin Carbon Films". Science. 306 (5696): 666–669. (22 October 2004)

[12] A. Eletskii, I. Iskandarova, A. Knizhnik, D. Krasikov, “Graphene: fabrication methods and thermophysical properties.” k Russian Research Centre `Kurchatov Institute'. Uspekhi Fizicheskikh Nauk 181 (3) 233 ± 268 (2011). DOI: 10.3367/UFNr.0181.201103a.0233

[13] A. Reina, X. Jia, J. Ho, D. Nezich, H. Son, V. Bulovic, M. Dresselhaus, J. Kong, "Large Area, Few-Layer Graphene Films on Arbitrary Substrates by Chemical Vapor Deposition". Nano Lett. 9, 30, (2009)

[14] C. Berger, et al. "Electronic confinement and coherence in patterned epitaxial graphene," Science 312, 1191–1196 (2006)

[15] A. Smith, K. Elgammal, et al. "Resistive graphene humidity sensors with rapid and direct electrical readout," Nanoscale, Royal Society of Chemistry (2015) DOI: 10.1039/C5NR06038A

[16] M. Chen, et al. "Fabrication of Humidity Sensor Based on Bilayer Graphene," IEEE Electron Device Letters 35:590-592, (2014)

[17] D. Zhang, J. Tong, B. Xia, Q. Xue, "Ultrahigh performance humidity sensor based on layer-by-layer self-assembly of graphene oxide/polyelectrolyte nanocomposite film," Sensors and Actuators B: Chemical. Vol 203, (2014)